



**ROBERT GORDON
UNIVERSITY ABERDEEN**

Utilization of hazardous materials in oil based mud waste to turn into value added polymeric nanocomposite materials

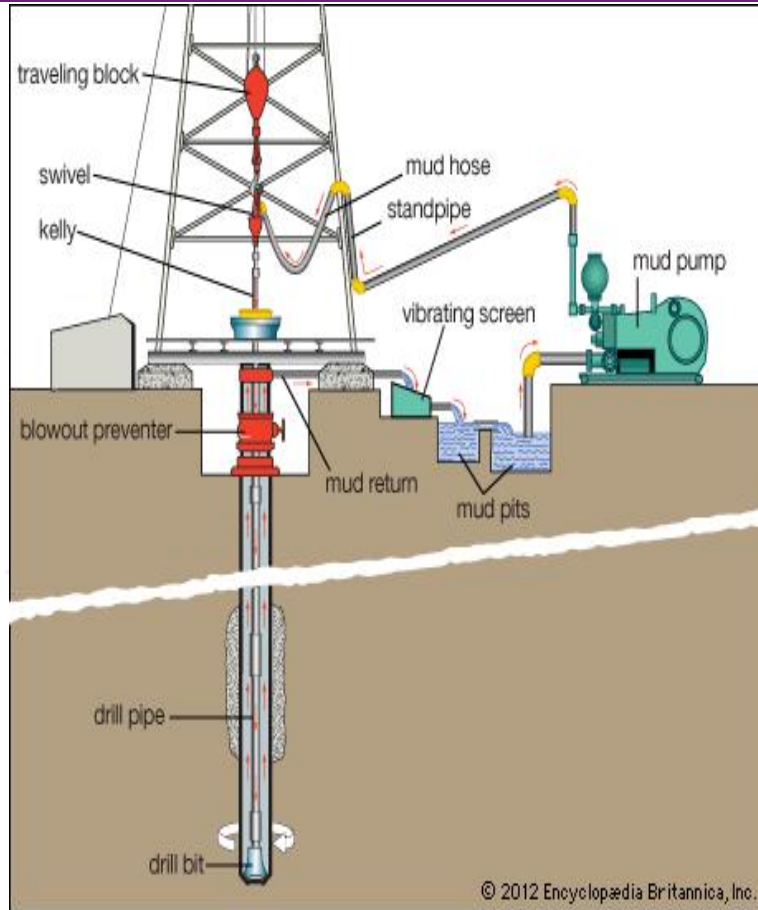
**Shohel Ahmed Siddique, Urenna V Adegbotolu, Kyari Yates,
James Njuguna**

E-mail: s.a.siddique@rgu.ac.uk, Tel: +44(0)1224 262310

Outline

- Background
- Aim & objectives
- Methodology
- Analysis
- Results discussion
- Conclusion

Background



Existing oil based mud (OBM) waste treatment methods

- Physical treatment
- Chemical process
- Biological process
- Thermal treatment

Fig. 1: The circulation of drilling mud during the drilling of an oil well.

Source: <https://www.britannica.com/technology/drilling-mud>

Existing OBM waste management options (based on cost, time, efficiency)

| Treatment | Time | Cost *(AUS\$) | Advantages | Disadvantages |
|---------------------------------------|---------------|-------------------------------|--|--|
| Composting | 56-8 days | 60-80 | useful by-product | air emission, fire risk |
| Land farming | 200-800 days | 10-12 | low cost | Environmental pollution |
| Land treatment | 400-1200 days | 4-5 | low cost | long-term monitoring |
| Bio augmented landfarming | 100-200 days | 15-20 | low cost | intense monitoring needed |
| Burial pit | 500-3000 days | 10-12 | on site treatment | long term monitoring needed |
| Landfills | 300-2500 days | 40-60 | relatively low cost | long term monitoring needed; legislative issues; slow biodegrading rates |
| Bio reactors | 10-30 days | 700 | rapid process | large cost; expertise needed; maintenance issues |
| Vermiculture | 28-56 days | 80-100 | useful by-product | suitable for a limited range of pollutants |
| Chemical solidification/stabilisation | 1-2 tonnes/h | 100-250 (plus disposal costs) | rapid process | large set-up cost; risk associated with long term stabilisation |
| Incineration | 5-6 tonnes/h | 500-1000 | waste reduction | large set-up and running cost; may not remove all pollutants |
| Thermal desorption | 3-10 tonnes/h | 400-1500 | waste reduction and low retention time | large set-up and running cost; |

Source: Ball AS, Stewart RJ, Schliephake K. A review of the current options for the treatment and safe disposal of drill cuttings. *Waste Manag Res* 2012 May;30(5):457-473.

Thermomechanical Cuttings Cleaner (TCC)

Sustainable
solution

???

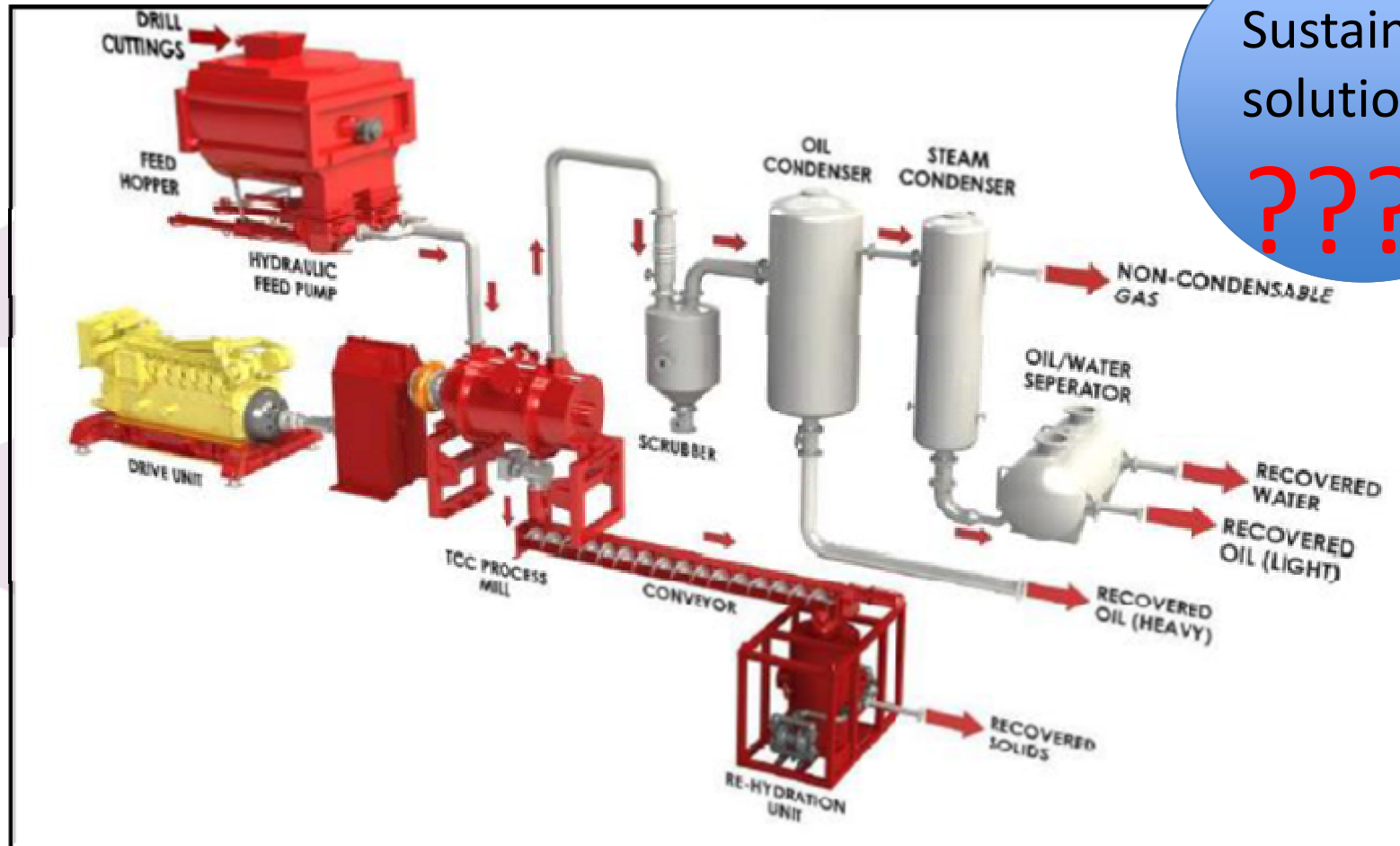
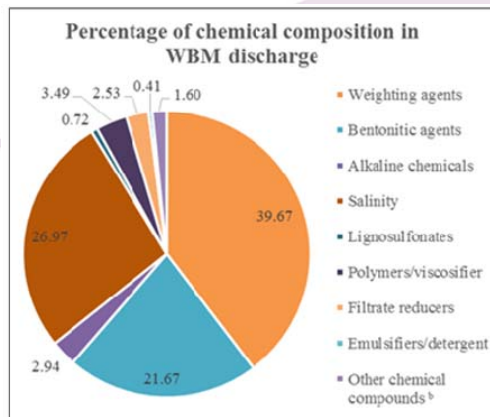
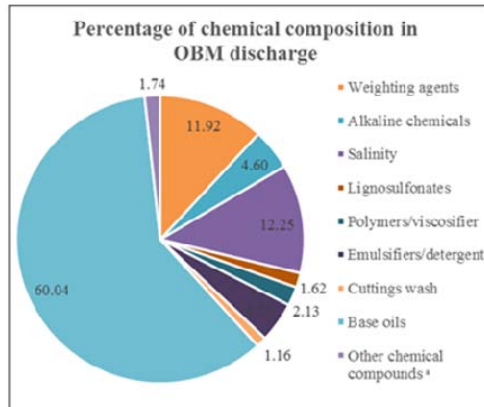


Fig. 2: Diagram of TCC system

Source: <http://www.halliburton.com/en-US/ps/baroid/fluid-services/waste-management-solutions/waste-treatment-and-disposal/thermal-processing-systems/thermomechanical-cuttings-cleaner-tcc.page>

OBM waste composition as a hazardous material



List I and II pollutants in environment

| Type of pollutants | Members of pollutant groups |
|--------------------|--|
| List I | Organohalogen compounds and substances |
| | Organophosphorus compounds |
| | Organotin compounds |
| | Carcinogenic substances |
| | Mercury and its compounds* |
| | Cadmium and its compounds* |
| | Persistent mineral oils and hydrocarbons of petroleum origin |
| | Persistent synthetic substances |
| | Certain metals, metalloids, and their compounds: 1) Zinc 2) Copper* 3) Nickel* 4) Chromium (Cr(VI))* 5) Lead* 6) Selenium* 7) Arsenic* 8) Antimony* 9) Molybdenum 10) Titanium 11) Th* 12) Barium 13) Beryllium 14) Boron 15) Uranium 16) Vanadium 17) Cobalt 18) Thallium* 19) Tellurium* 20) Silver |
| | Biocides and their derivatives |
| List II | Toxic or persistent organic compounds of silicon and its substances |
| | Inorganic compounds of phosphorus and elemental phosphorus |
| | Non persistent mineral oils and hydrocarbons of petroleum origin |
| | Cyanides and fluorides |
| | Substances causing oxygen imbalance such as ammonia, nitrites |

*: Hazardous waste classified in according to Directive 2008/98/EC

Fig. 3: Percentage of individual chemical constituents present in OBM and WBM discharge adapted from Hudgins .

Source: Siddique S, Kwoffie L, Addae-Afoakwa K, Yates K, Njuguna J. Oil Based Drilling Fluid Waste: An Overview on Environmentally Persistent Pollutants. In IOP Conference Series: Materials Science and Engineering 2017 May (Vol. 195, No. 1, p. 012008). IOP Publishing.

Aim and Objectives

Aim:

To understand and evaluate the crystallinity and thermal degradation behaviour of PA6 nanocomposites using reclaimed clay from oil based drilling fluids waste.

Objectives

1. Morphology investigation of PA6/OBMFs nanocomposites using SEM.
2. Elemental analysis of PA6/OBMFs nanocomposites using EDXA.
3. Chemical structure analysis using FTIR technique.
4. PA6/OBMFs nanocomposites decomposition study using TGA.
5. Degradation study of PA6/OBMFs nanocomposites using DSC.

Methodology

Materials and experiments

➤ Matrix material

- PA6

➤ Nanofiller

- OBMFs (Thermally treated)

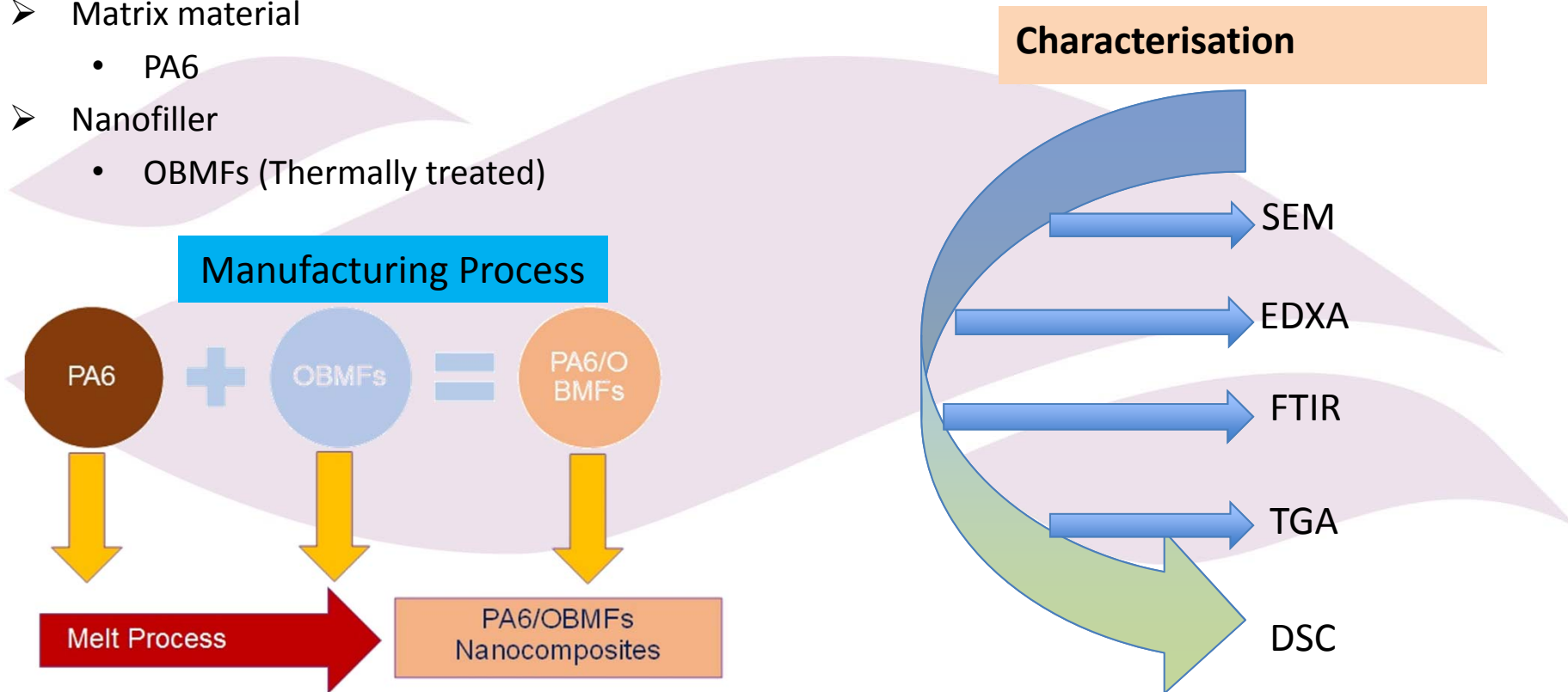


Fig. 4: Schematic representation of (a) PA6/ OBMFs nanocomposite manufacturing process and (b) different experimental analysis of PA6/ OBMFs nanocomposite.

SEM analysis

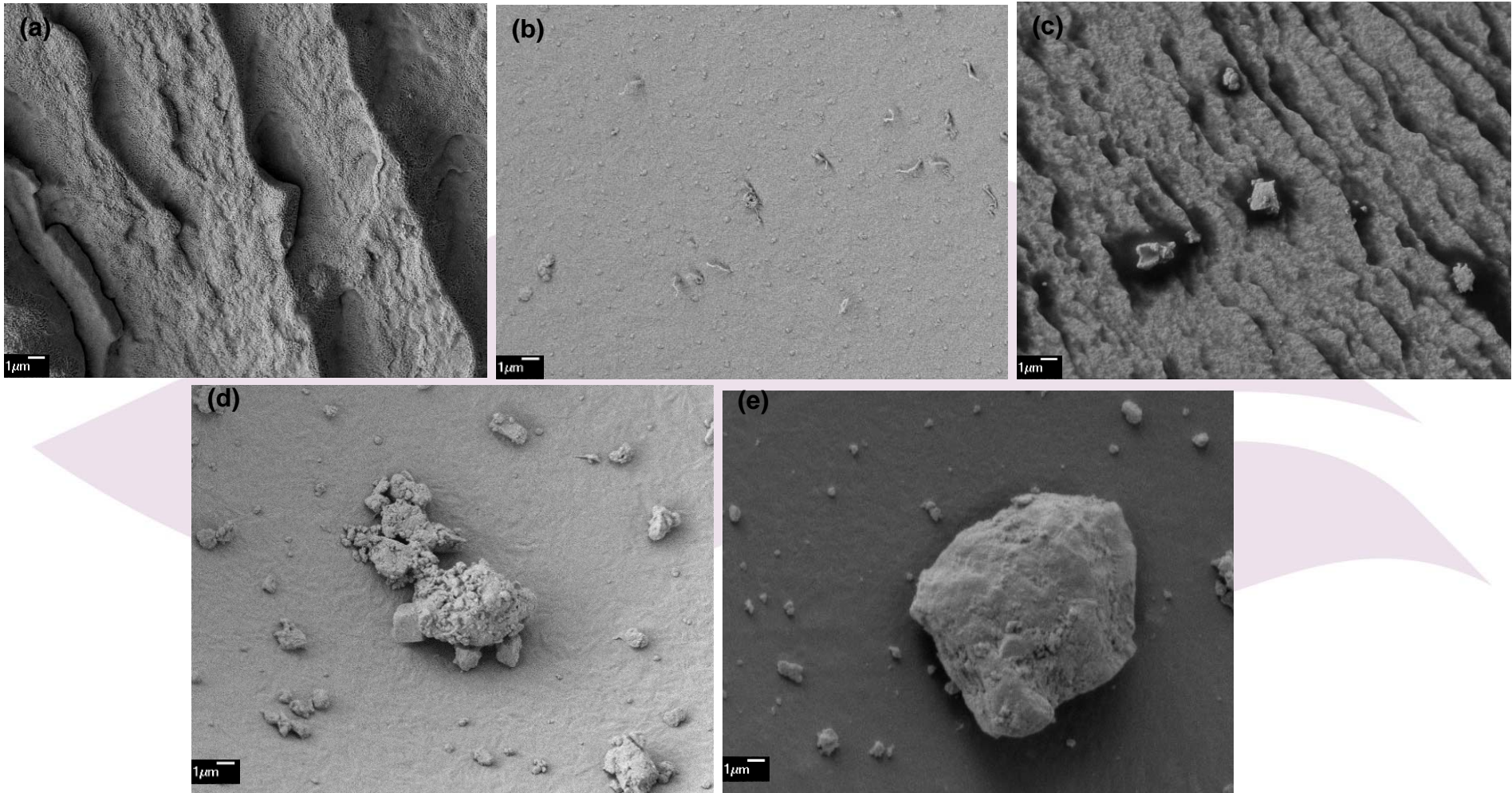


Fig. 5: SEM images of (a) PA6; (b) PA6 with 2.5 wt% OBMFs; (c) PA6 with 5.0 wt% OBMFs; (d) PA6 with 7.5 wt% OBMFs; and (e) PA6 with 10.0 wt% OBMFs.

EDXA analysis

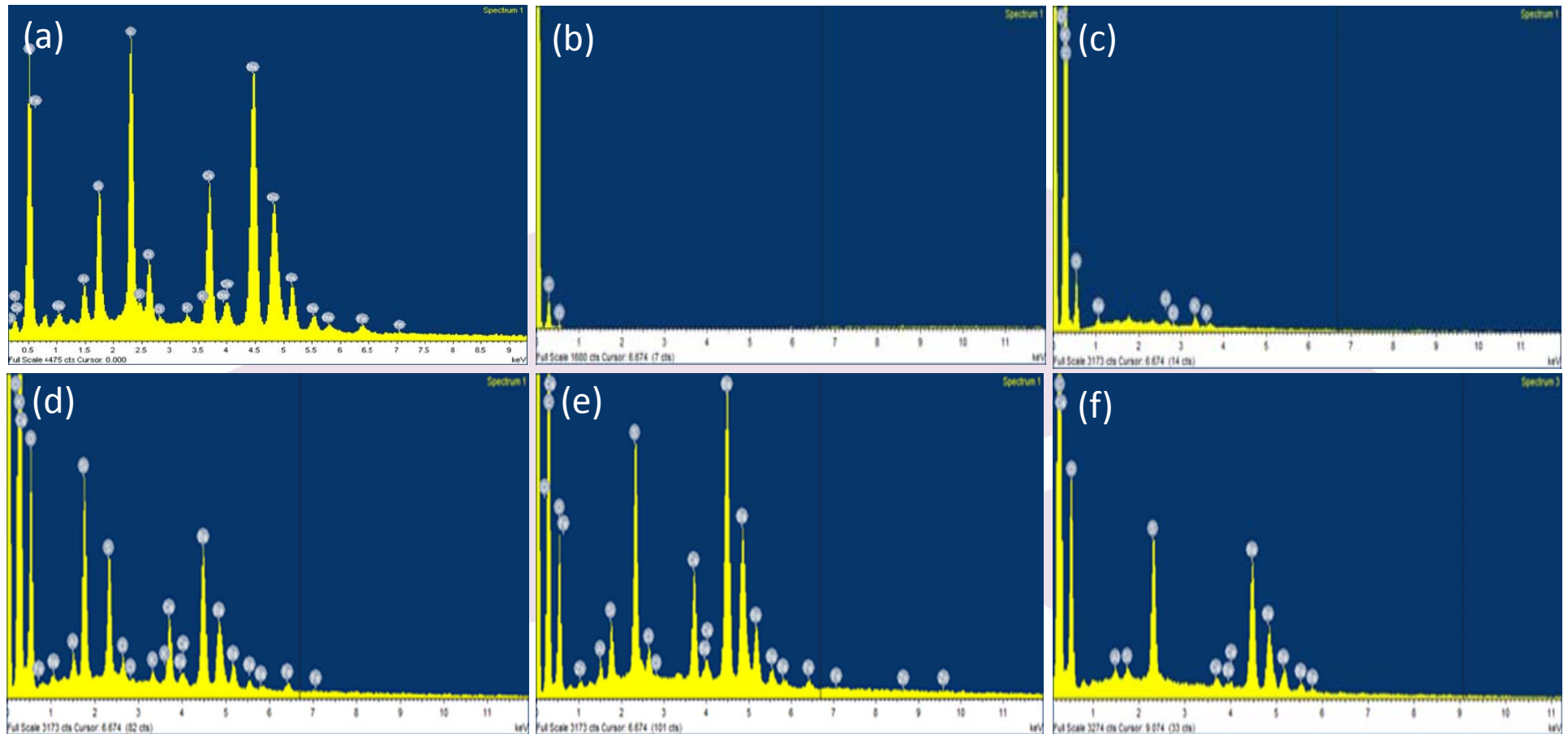


Fig. 6: EDX spectra of (a) OBMFs; (b) PA6; (c) PA6+2.5 wt% OBMFs; (d) PA6+5.0 wt% OBMFs; (e) PA6+7.5 wt% OBMFs and (f) PA6+10.0 wt% OBMFs.

FTIR analysis:

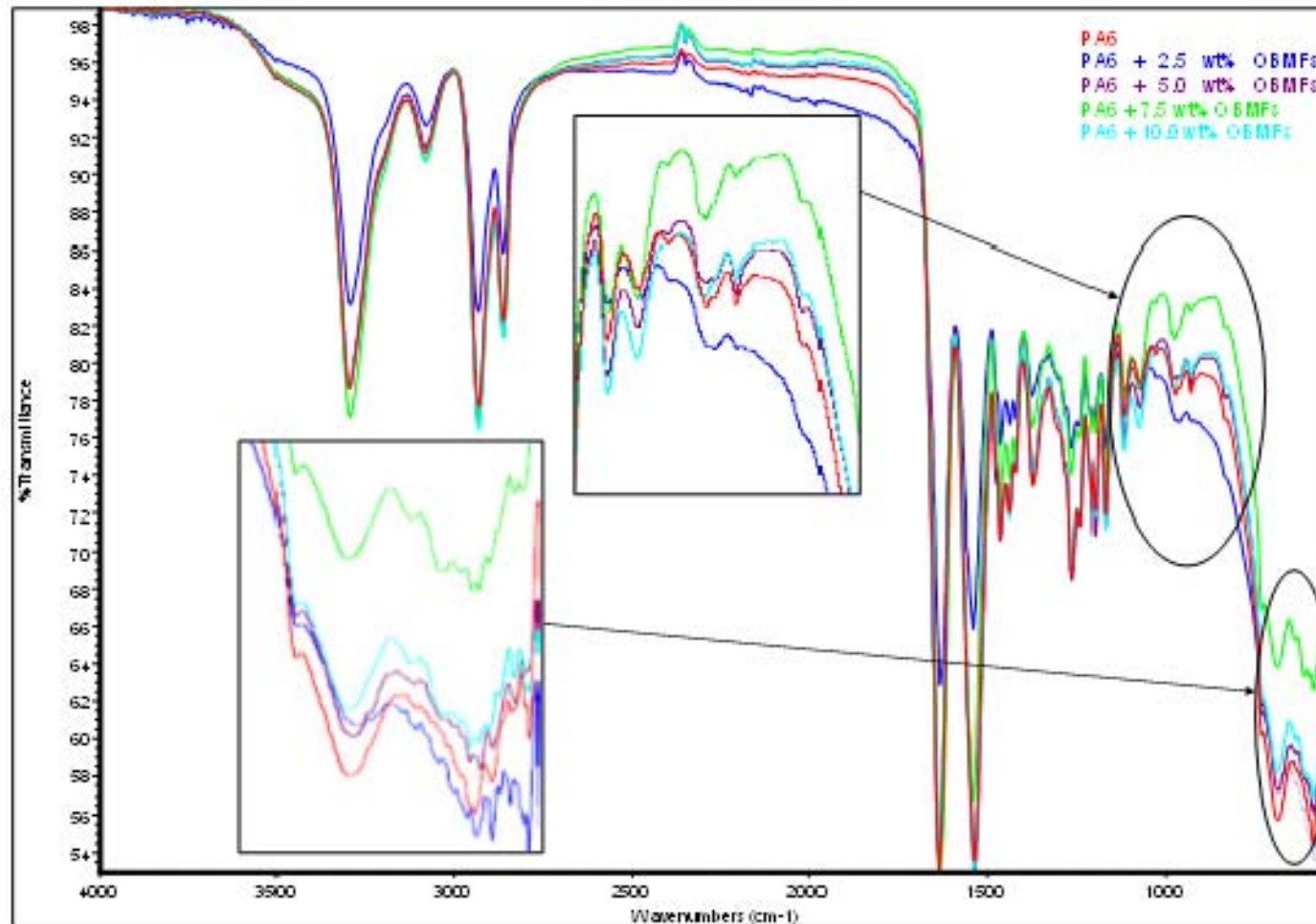


Fig. 7: Comparison of FTIR full scale spectra of PA6 and its nanocomposite.

ATR FT-IR peak assignments

| Wave number (cm ⁻¹) | Assignments |
|---------------------------------|------------------------------------|
| 3295 | Hydrogen-bonded N-H stretching |
| 3079 | Fermi-resonance of N-H stretching |
| 2930 | V _{as} (CH ₂) |
| 2859 | V _s (CH ₂) |
| 1633 | Amide I |
| 1539 | Amide II |
| 1462 | CH ₂ deformation |
| 1435 | CH ₂ deformation |
| 1370 | Amide III & CH ₂ wag |
| 1259 | Amide III & CH ₂ wag |
| 1200 | Amide III & CH ₂ wag |
| 1169 | CO-NH, skeletal motion (Am) |
| 1118 | C-C stretching (Am) |
| 1074 | C-C stretch (Am) |
| 973 | CO-NH in plane vibration |
| 680 | Amide V |
| 525-580 | Primary aliphatic nitriles (C≡N) |

Decomposition behaviour of PA6 and its nanocomposite

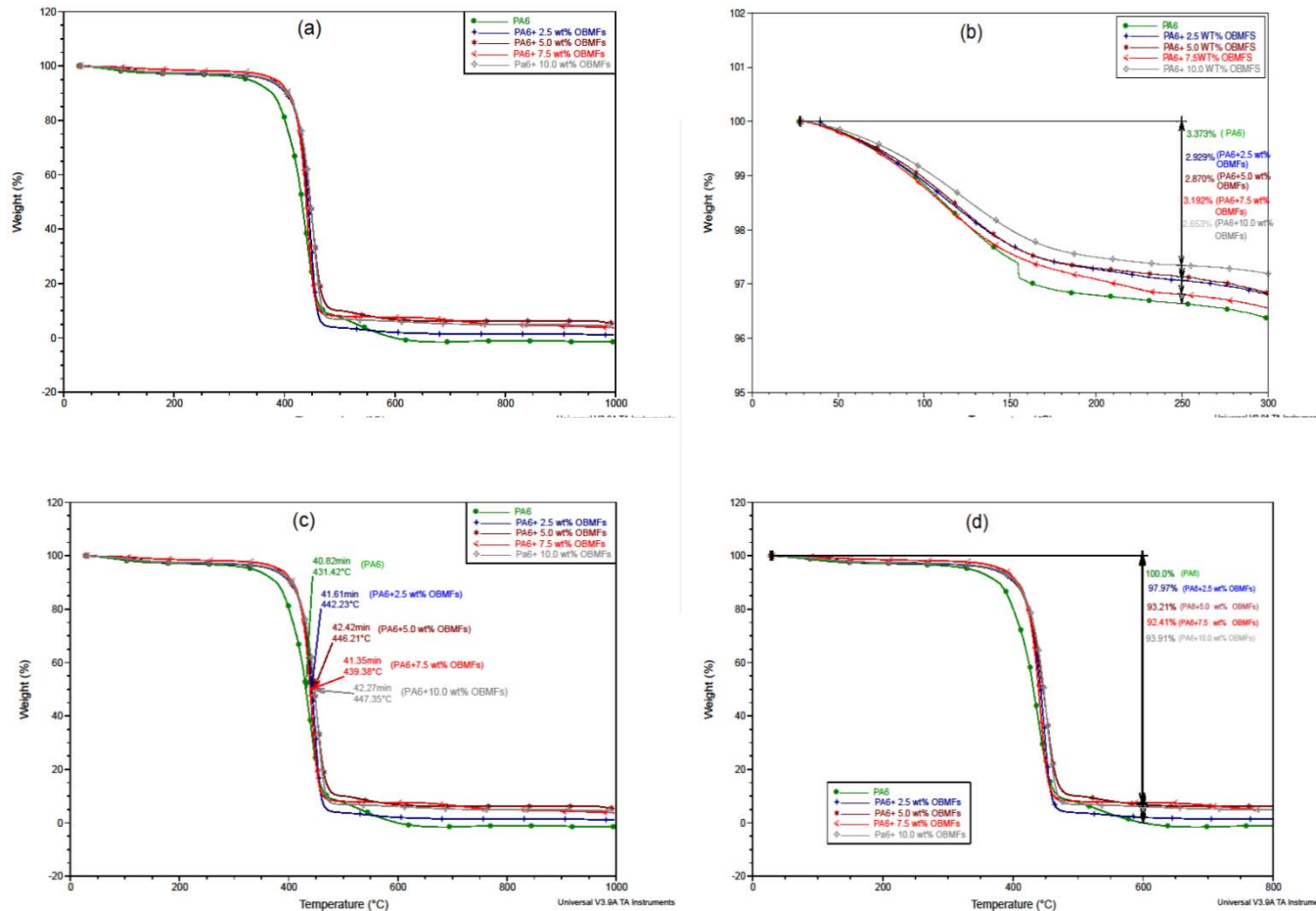


Fig. 8: TGA of PA6 and PA6/OBMFs nanocomposites at: (a) complete thermograms of all samples; (b) 250°C; (c) D ½; (d) 600 °C.

TGA analysis at different decomposition stages of PA6 and its nanocomposites

| Material | % wt loss at 250 °C | T _{D10%} (° c) | T _{D50%} (° c) | D 1/2 Time | Residue (% wt) at 600 °C |
|--------------------|---------------------|-------------------------|-------------------------|--------------|--------------------------|
| PA6 | 3.37 | 399.24 | 431.42 | 40.82 | 0.00 |
| PA6+2.5 wt% OBMFs | 2.93 | 407.77 | 442.23 | 41.61 | 2.03 |
| PA6+5.0 wt% OBMFs | 2.87 | 416.87 | 446.21 | 42.42 | 6.79 |
| PA6+7.5 wt% OBMFs | 3.19 | 412.32 | 439.38 | 41.35 | 7.59 |
| PA6+10.0 wt% OBMFs | 2.65 | 416.87 | 447.35 | 42.27 | 6.09 |

Degradation behaviour of PA6 and its nanocomposite

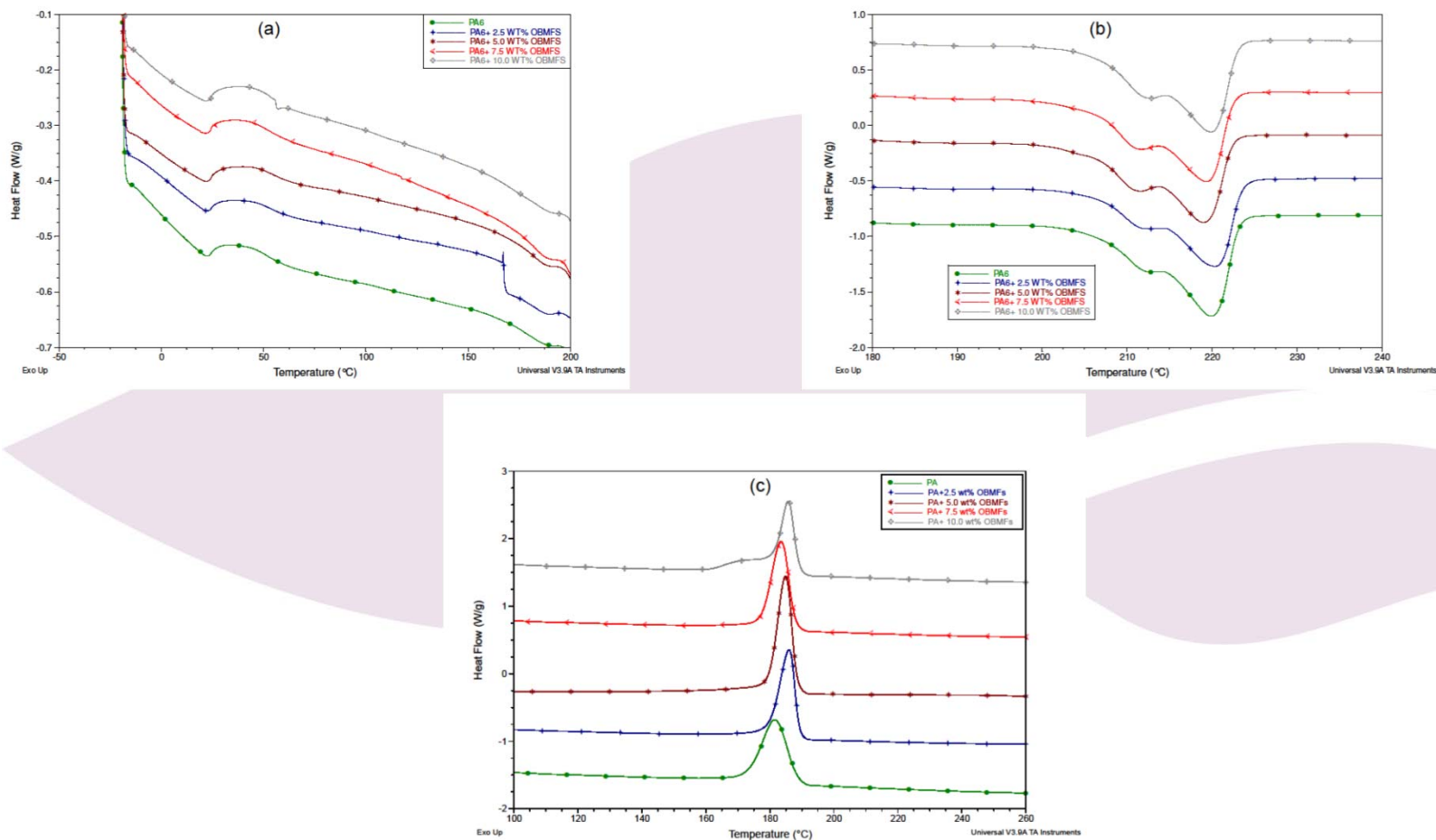


Fig. 9: DSC thermograms of PA6 and its nanocomposites at (a) T_g , (b) T_m and (c) T_c .

% of crystallinity calculation

$$\% \text{ crystallinity} = [\Delta H_m - \Delta H_c] / \Delta H_m^0 * 100\%$$

| Material | ΔH_m (J/g) | ΔH_c (J/g) | $\Delta H_m - \Delta H_c$ (J/g) | $((\Delta H_m - \Delta H_c) / \Delta H_m^0) * 100\%$ |
|--------------------|--------------------|--------------------|---------------------------------|--|
| PA6 | 52.83 | 0 | 52.83 | 22.96 |
| PA6+2.5 wt% OBMFs | 48.05 | 0 | 48.05 | 20.88 |
| PA6+5.0 wt% OBMFs | 49.32 | 0 | 49.32 | 21.43 |
| PA6+7.5 wt% OBMFs | 51.56 | 0 | 51.56 | 22.41 |
| PA6+10.0 wt% OBMFs | 50.73 | 0 | 50.73 | 22.05 |

Heat Capacity Calculation

$$C_p = (\delta Q / \delta t) \times (\delta t / \delta T)$$

| Material | Mass of samples (m) mg | Heat capacity (J/g) | Specific heat capacity (Cp) Jk ⁻¹ kg ⁻¹ |
|--------------------|------------------------|---------------------|---|
| PA6 | 6.20 | 60.57 | 2523 |
| PA6+2.5 wt% OBMFs | 6.30 | 55.87 | 2327 |
| PA6+5.0 wt% OBMFs | 6.30 | 57.66 | 2402 |
| PA6+7.5 wt% OBMFs | 7.80 | 60.55 | 2522 |
| PA6+10.0 wt% OBMFs | 6.30 | 64.69 | 1321 |

Schematic diagram of RAF and MAF

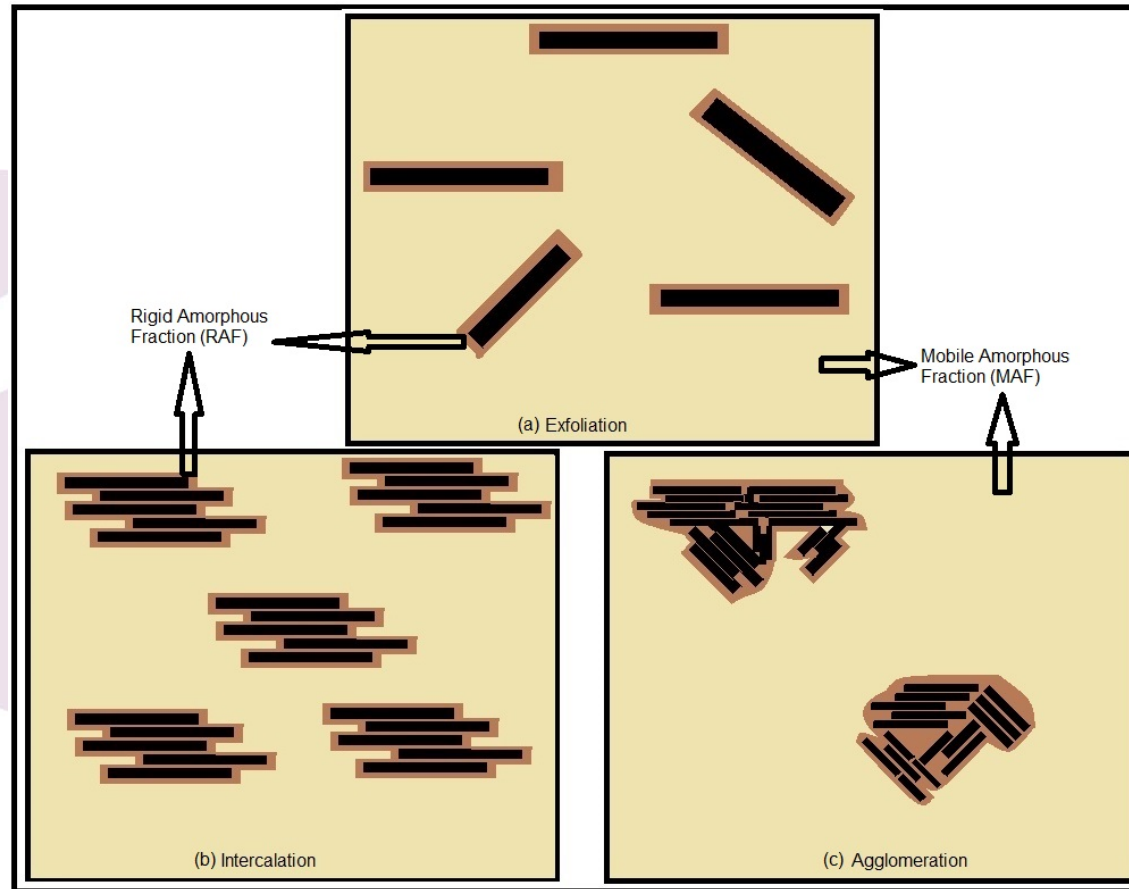


Fig. 10: Schematic diagram of OBMFs platelets associated with MAF and RIF of PA6 matrix

RAF and MAF Calculation

$$MAF = (\Delta C_p / \Delta C_p(am)) * 100\%$$

$$RAF = 1 - \text{crystallinity} - \Delta C_p / \Delta C_{p \text{ pure}}$$

or

$$RAF' = 1 - \text{filler content} - \Delta C_p / \Delta C_{p \text{ pure}}$$

| Material | MAF | CF | CF' | RAF= 100-MAF-CF | RAF'= 100-MAF-CF' | TIF |
|--------------------|-------|-------|-------|-----------------|-------------------|-------|
| PA6 | 27.26 | 22.96 | 0.00 | 49.78 | 72.74 | 72.74 |
| PA6+2.5 wt% OBMFs | 27.46 | 20.88 | 2.50 | 51.66 | 70.04 | 72.54 |
| PA6+5.0 wt% OBMFs | 58.91 | 21.43 | 5.00 | 19.66 | 36.09 | 41.09 |
| PA6+7.5 wt% OBMFs | 46.01 | 22.41 | 7.50 | 31.58 | 46.49 | 53.99 |
| PA6+10.0 wt% OBMFs | 55.04 | 22.05 | 10.00 | 22.91 | 34.96 | 44.96 |

Relation between TIF and filler dispersion

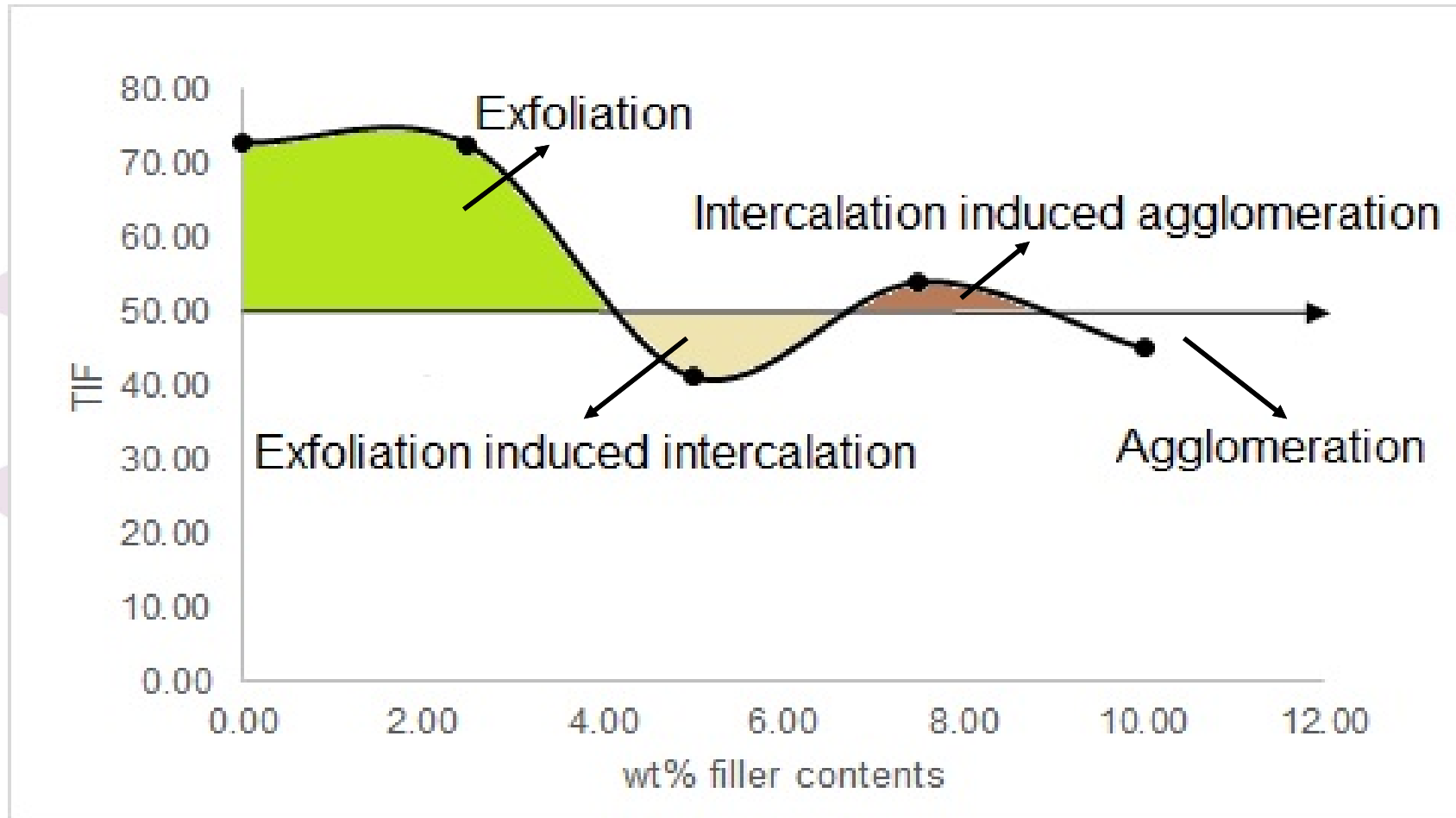


Fig. 11: Relation between TIF and dispersion behaviour of OBMFs in PA6 matrix

Conclusion

- In TGA, the % weight loss of PA6/OBMFs nanocomposites decreases with the incremental weight % of OBMFs in PA6/OBMFS nanocomposites
- There is not any significant heat capacity property changes for PA6 with 2.5 wt%, 5.0 wt% and 7.5 wt% OBMFs nanocomposites
- There is a drastically heat capacity (about 47%) reduction noticeable for PA6 with 10.0 wt% nanocomposite
- 50% TIF line deduce the degree of dispersity in PA6/OBMFs nanocomposites



Thank You